

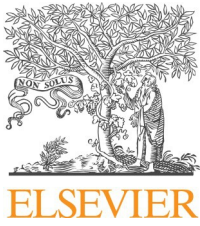
Central Lancashire Online Knowledge (CLoK)

Title	Particle release from dental implants immediately after placement - An ex vivo comparison of different implant systems.
Type	Article
URL	https://clock.uclan.ac.uk/id/eprint/41924/
DOI	https://doi.org/10.1016/j.dental.2022.04.003
Date	2022
Citation	Barrak, Fadi N, Li, Siwei, Muntane, Albert, Bhatia, Manoj, Crossthwaite, Kathryn Nicola and Jones, Julian (2022) Particle release from dental implants immediately after placement - An ex vivo comparison of different implant systems. <i>Dental materials</i> , 38 (6). pp. 1004-1014. ISSN 0109-5641
Creators	Barrak, Fadi N, Li, Siwei, Muntane, Albert, Bhatia, Manoj, Crossthwaite, Kathryn Nicola and Jones, Julian

It is advisable to refer to the publisher's version if you intend to cite from the work.
<https://doi.org/10.1016/j.dental.2022.04.003>

For information about Research at UCLan please go to <http://www.uclan.ac.uk/research/>

All outputs in CLoK are protected by Intellectual Property Rights law, including Copyright law. Copyright, IPR and Moral Rights for the works on this site are retained by the individual authors and/or other copyright owners. Terms and conditions for use of this material are defined in the <http://clock.uclan.ac.uk/policies/>

Available online at www.sciencedirect.com

ScienceDirect

journal homepage: www.elsevier.com/locate/dental

Particle release from dental implants immediately after placement – An ex vivo comparison of different implant systems

Fadi Barrak^{a,b,1}, Siwei Li^{a,1}, Albert Muntane^b, Manoj Bhatia^b,
Kathryn Crossthwaite^b, Julian Jones^{a,*}

^a Department of Materials, Imperial College London, SW7 2AZ, UK

^b School of Dentistry, University of Central Lancashire, PR1 2HE, UK

ARTICLE INFO

Article history:

Received 7 April 2021

Received in revised form 14 March 2022

Accepted 1 April 2022

Key words:

Dental implant

Particle release

Wear

Commercial pure titanium

Titanium alloy

Ti-6Al-4V

Toxicity

Roxolid

Phagocytosis

ABSTRACT

Objectives: Metallic element release during implant placement can lead to mucositis and peri-implantitis. Here, using ex vivo porcine mandibles, the release of metallic elements into the surrounding bone with different material and geometrical designs was quantified. **Methods:** Implants from BioHorizons® and Straumann® (Bone level, tapered/cylindrical, 3/4 mm body diameter, Ti-CP4/Ti-6Al-4V/Ti-15Zr) systems were used. Micro computed tomography and inductively coupled plasma optical emission spectroscopy was used to visualise and quantify metallic elements in bone, following acid digestion. Implant surfaces were examined with scanning electron microscopy and internalization of implant particles by human gingival fibroblasts (HGFs) and RAW 264.7 macrophages were demonstrated in vitro.

Results: Implants with wider body diameters resulted in higher metallic element release. Ti-6Al-4V implants released significantly more metallic elements in comparison to both Ti-CP4 and Ti-15Zr devices with similar design and dimensions. Tapered Ti-CP4 implants released less compared to those with cylindrical design. All three types of particles were internalized by HGFs and RAW 264.7.

Significance: Ti-CP4 and Ti-15Zr appear to be more suitable materials, however, further studies are required to elucidate the biological effects of the fine particles and/or metallic species from dental implants. Authors would like to raise the awareness in the dental profession community that careful evaluation of the materials used in dental implants and

Abbreviations: IL-1 β , Interleukin 1 beta; IL-6, Interleukin 6; TNF- α , Tumour necrosis factor alpha; Ti-6Al-4V, Grade 5 titanium alloy; Ti-CP4, Commercial pure titanium; Ti-15Zr, Roxolid® titanium alloy; ICP-OES, Inductively coupled plasma optical emission spectrometer; DLS, Dynamic light scattering; μ CT, Micro computed tomography; SEM, Scanning electron microscopy; Ti, Titanium; V, Vanadium; Al, Aluminum; Zr, Zirconium; Fe, Iron; HGF, Human gingival fibroblasts; FBS, Fetal bovine serum; FITC, Fluorescein 5(6)-isothiocyanate; PBS, Phosphate-buffered saline; DAPI, 4',6-diamidino-2-phenylindole; S.D, Standard deviation; DNA, Deoxyribonucleic acid; miRNA, Micro ribonucleic acid; DMEM, Dulbeccos's modified Eagle's medium

* Correspondence to: Department of Materials, Imperial College London, South Kensington Campus, SW7 2AZ, UK.

E-mail addresses: fbarrak@visitingsspecialistservices.co.uk (F. Barrak), siwei.li@vssacademy.co.uk (S. Li), albertmuntane@gmail.com (A. Muntane), mbimplants@gmail.com (M. Bhatia), julian.r.jones@imperial.ac.uk (J. Jones).

¹ Both authors contributed equally

<https://doi.org/10.1016/j.dental.2022.04.003>

0109-5641/© 2022 The Authors. Published by Elsevier Inc. on behalf of The Academy of Dental Materials.

CC_BY_4.0

the potential risks of the individual constituents of any alloy are needed. The potential cytotoxicity of Ti-6Al-4V implant particles should be highlighted. Further investigations on the biological effect of the fine particles or metallic species released from dental implants are also needed.

© 2022 The Authors. Published by Elsevier Inc. on behalf of The Academy of Dental Materials.
CC_BY_4.0

1. Introduction

Titanium and titanium based alloys are the most widely used metallic materials for orthopaedic and dental implants [1]. Orthopaedic loosening and oral peri-implantitis remain a major post-operative concern [2]. In Dentistry, peri-implantitis, which is classified as inflammation of the soft gum tissue and loss of alveolar bone, is the main cause of implant failures. Peri-implantitis has long been believed to have a microbial etiology, but more recently has been associated with aseptic inflammation around an implant due to the release of metallic particles and ions from the implants [3–5]. Particle production is likely as implants, especially those with finely roughened surface, are screwed into bones. Surface degradation of the implant body can be accelerated by a number of factors such as wear and corrosion [4–6]. Once onset of peri-implantitis occurs, it is difficult to control, due to the lack of well-established treatment protocols, resulting in bone resorption and implant loss [7].

Although titanium-based prostheses are considered biocompatible (non-toxic), particles and ions released from them may not be. The implants are considered biocompatible because cell death (necrosis) around implants over short time scales is negligible and they pass *in vitro* cytotoxicity tests, such as ISO-10993, as they do not release “leachants” on immersion in cell culture studies. Fibrous encapsulation occurs when nearly inert implants are too large for phagocytosis. If particles are produced, they may be small enough for internalization by macrophages, causing frustrated phagocytosis and local chronic inflammation, which can lead to osteolysis in the surrounding bone [8].

Previous studies observed the size of particles produced from titanium-based dental implants to range from nanometre to micrometre scales [5,9,10]. Biopsies of soft tissue around failing dental implants (titanium and titanium alloys) revealed inflammatory reactions around aggregates of particles, which have been traditionally classed as ‘wear particles’ [11,12]. Several studies have reported potential sources of metallic particles and ions in Implantology, e.g., from the implant surfaces during placement and from the implant-abutment interface during functional loading. Particularly, at the moment of implant placement, the shear force originated from the frictional movements at implant-bone interface can incur both chemical and topographical changes on the implant surface, which result in the release of particles [13,14].

Particles from orthodontic mini-implants (and orthopaedic implants) have also been recorded in lungs, liver, spleen and bone marrow [15,16]. Titanium dioxide particles and particles released from ultrasonic scaling of Grade 5 titanium alloy (an alloy consists of titanium, aluminum and

vanadium, Ti-6Al-4 V) implants have been reported both *in vitro* and in animal models to induce marked upregulation of pro-inflammatory markers including interleukin 1 beta (IL-1 β), IL-6 and tumour necrosis factor alpha (TNF- α) in macrophages, leading to inflammation-induced osteoclastogenesis and bone resorption (osteolysis) [17]. The activation of the innate immune system leads to periprosthetic osteolysis and subsequent implant failure, resulting in the need of an additional surgery for patients [18,19]. As particle size decreases, specific surface area increases, which can increase the rate of ion release. We recently found that vanadium ion dissolution from Ti-6Al-4V can cause toxicity [10].

The aim of this study was to systematically evaluate the impact of implant material composition and geometrical design of the implant on the quantity of metallic products released from dental implants immediately after placement in an *ex vivo* pig mandible bone model. Internalization of such particles by peri-implant cell populations *in vitro* was also investigated. All implant materials were bone level implant designs. Metals were: Ti-CP4 (commercially pure titanium); Ti-15Zr (titanium-zirconium alloy); and Ti-6Al-4V (Titanium-6%Aluminum-4%Vanadium alloy). Geometries were cylindrical or tapered.

2. Materials and methods

Reagents and solvents were purchased from Sigma-Aldrich (Dorset, UK) and Thermo Fisher Scientific (Paisley, UK). Implants were purchased from Straumann (Crawley, UK) and BioHorizons (Bracknell, UK). Pig mandibles were purchased from Medical Meat Supplies (Oldham, UK). No ethical clearance was required. Ti-15Zr particles were created from Roxolid® disks provided by Straumann (Basel, Switzerland). Ti-CP4 and Ti-6Al-4V particles (produced from Ti-CP4 and Ti-6Al-4V implant material blocks) were gifted from Dr Jonathan Jeffers (Imperial College London). Particle sizes were determined using Malvern Mastersizer and dynamic light scattering (DLS).

2.1. Implants and surgical instruments

The specifications of the implant systems used in this study are presented in Table 1. Straumann implants with parallel/cylindrical and tapered walls, consisting of grade 4 and Roxolid at diameters of 3.3 and 4.8 were used. Nearest comparable systems from BioHorizons were used. Drills and surgical handpiece protocols were set in accordance to manufacturer instructions for each implant system. A diamond disc was used to cut and prepare bones for analyses following implant placement.

Table 1 – Specifications of implant systems used and their mass loss into the bone after implantation. All implants were bone level type with an endosteal length of 12 mm. Straumann® implants have the same platform and transfer piece. The nearest comparable systems from BioHorizons® was used. Each model and size were given an ID in this study. Ti-CP4 refers to commercially pure titanium; Ti-15Zr refers to titanium, zirconium alloy; Ti-6Al-4V refers to Titanium-6%Aluminum-4%Vanadium alloy. SLA® is a proprietary Straumann® implant surface created using technique based on large-grit sandblasting and acid-etching. Laser-Lok®/RBT is a BioHorizons® proprietary surface created using laser ablation with resorbable blast texturing.

Brand	Model no.	Implant type	Material	Surface	Endosteal diameter (mm)	ID in this study	Mass loss after implantation (estimated, µg)
Straumann®	21.2612	Cylindrical	Ti-CP4	SLA®	3.3	BL3	554.1 ± 14.6
Straumann®	21.6612	Cylindrical	Ti-CP4	SLA®	4.8	BL4	660.9 ± 15.4
Straumann®	21.3412	Tapered	Ti-CP4	SLA®	3.3	BL-T-S3	134.3 ± 12.7
Straumann®	21.6412	Tapered	Ti-CP4	SLA®	4.8	BL-T-S4	518.5 ± 14.6
Straumann®	21.3512	Tapered	Roxidid® (Ti-15Zr)	SLA®	3.3	BL-T-R3	448.1 ± 35.4
Straumann®	21.6512	Tapered	Roxidid® (Ti-15Zr)	SLA®	4.8	BL-T-R4	548.4 ± 38.3
BioHorizons®	TLX3412	Tapered	Ti-6Al-4V	Laser-Lok®/RBT	3.4	BH3	639.1 ± 53.6
BioHorizons®	TLX4612	Tapered	Ti-6Al-4V	Laser-Lok®/RBT	4.6	BH4	690.5 ± 15.1

2.2. Implant placement

Pig mandible was used for implant insertion. Each mandible sample was divided into 3 regions (Fig. 1): (1) untreated bone control (n = 5); (2) drill only control (n = 5); and (3) implant placement (n = 5). In the area of drill only controls, the bone was prepared with implant drills without implant placement to ensure the drilling was not contributing metallic particles. The preparation was done in accordance with each implant system's surgical protocol as provided by the manufacturer. Physiological saline solution (Hygitech, London, UK) was used to provide cooling during the drilling and implant placement procedure. Following drilling and implant placement, mandible bones were cut into 3 parts based on the above description using a micro bone saw (diamond disc). Each bone section was then sectioned vertically, in half, to allow the removal of implant. Bone samples were collected and stored at -20 °C until used for further analyses. Samples for micro computed tomography (µCT) scanning and scanning electron microscopy analyses were fixed in 4% paraformaldehyde and stored at 4 °C.

2.3. Bone and particle digestion

Collected bone samples were acid digested using protocols described previously [20]: each sample was submerged overnight in 5 mL of digestion acid (4 parts 65% nitric acid to 1 part 96% sulfuric acid) in screw-capped polypropylene tubes at 40 °C over a water bath in a safety fume hood. The caps were pierced to allow acid fumes to escape. The temperature was then increased to 70 °C for 2 h and again to 95 °C for further 1 h. The resulting solutions were allowed to cool to room temperature before carefully mixed and centrifuged to sediment any residuals. The clear supernatants were collected for further analyses. Implant particles (Ti-CP4, Ti-6Al-4V and Ti-15Zr) with known quantity (0.75 mg, 1.5 mg and 3 mg) were also digested using the same method for the generation of Ti release standard curve, which was subsequently used for the approximation of the wear particle quantities.

2.4. Inductively coupled plasma optical emission spectrometer (ICP-OES)

The elemental concentration of titanium, aluminum, iron and vanadium in the digested solution was determined using ICP-OES. 1 mL of each sample was diluted to 10 mL with deionized water and filtered through a 0.2 µm membrane. Mixed standards of titanium (Ti), aluminum (Al), iron (Fe) and vanadium (V) ions were prepared at 0, 2, 5, 20 and 40 ppm for calibration. All samples were run in triplicates. Final elemental concentration was normalised against untreated bone controls.

2.5. Scanning electron microscopy (SEM)

Collected implants were dried in a 60 °C oven and secured to an aluminum sample holder with carbon tape and coated with 10 nm gold. Secondary electron images were acquired

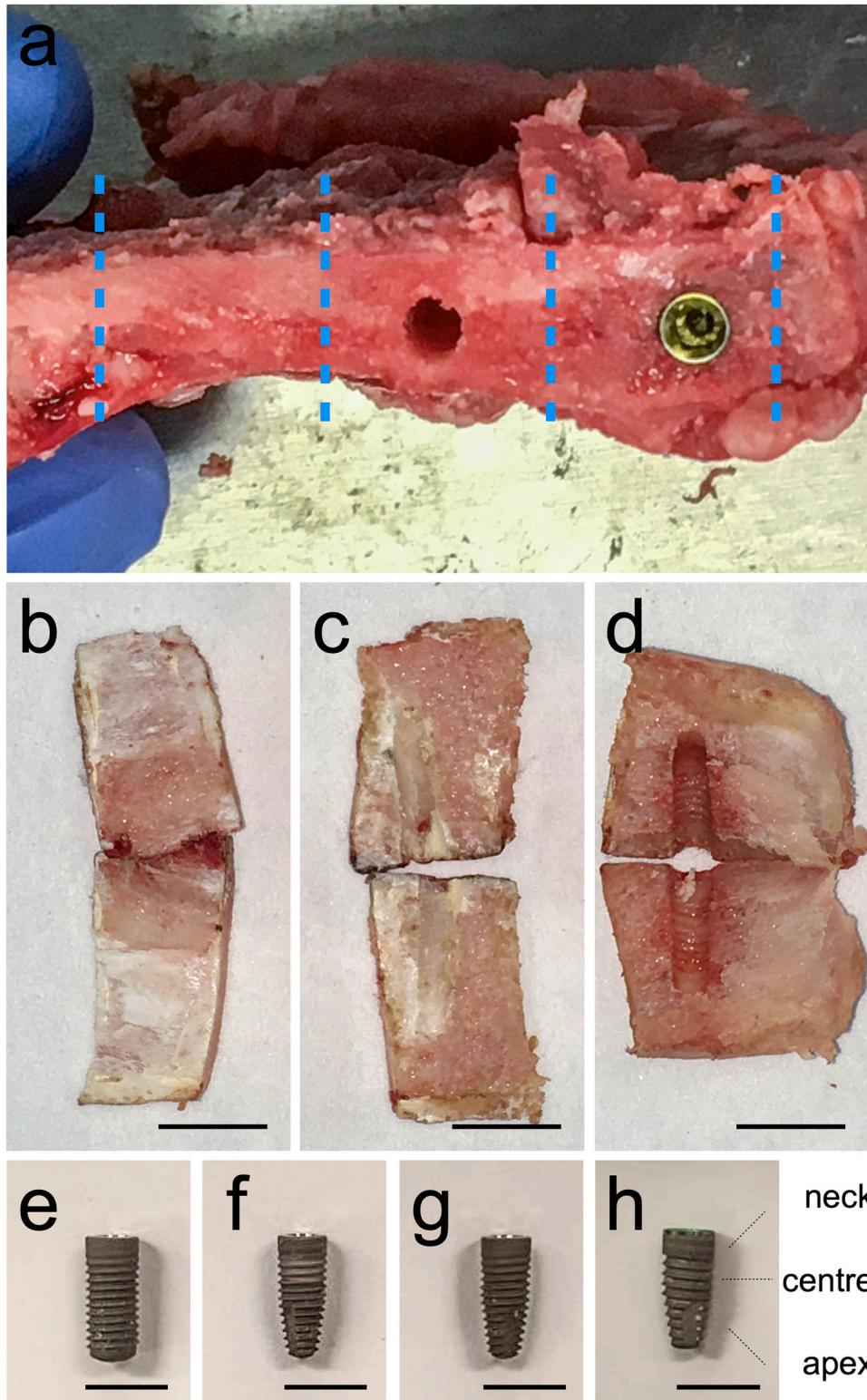


Fig. 1 – Representative photographs of implant placement in the *ex vivo* pig mandible model. (a) Each mandible sample was divided into three regions: bone control, drill only and implant placement. Following implant placement, mandible bones were cut into the three parts: untreated bone control (b), drill only (c) and implant placement (d) and sectioned vertically in half to allow removal of implant. Representative image of implants following placement and removal: (e) Straumann Ti-CP4 cylindrical (BL); (f) Straumann Ti-CP4 tapered (BLT-S); (g) Straumann Ti-15Zr tapered (BLT-R) and (h) BioHorizon Ti-6Al-4 V tapered (BH). In the drill only area, bone was prepared with implant drills without implant placement. Scale bars are 1 cm.

using Zeiss Sigma-300 scanning electron microscope with accelerating voltage of 5 kV.

2.6. Three-dimensional micro-computed tomography (μ -CT)

A Zeiss Versa 520 X-Ray scanner (Zeiss, Germany) was used to detect metal particles in bone samples (as shown in Fig. 1, dimensions of $\sim 1.5 \times 1.5 \times 1.5$ cm) following placement and removal of implants. The following settings were used: 140 kV voltage, 71 μ A current (with high efficiency filter), 12.3 μ m voxel size, 0.4 \times optical magnification, 5 s exposure time, 2.5 MHz camera readout, 1 recon binning and 1601 projections. μ -CT projections were reconstructed within the Zeiss Scout-and-Scan Control System. Reconstructed 3-D volumes were visualised and analyzed using Fiji ImageJ software (version 1.52p, NIH, USA). No further image adjustment, enhancement or filtering was applied.

2.7. Cell culture experiments

2.7.1. Cellular uptake of implant particles

To demonstrate cellular uptake of implant particles, human gingival fibroblasts (HGFs) (ATCC, Middlesex, UK) and murine RAW 264.7 macrophage cell line (Sigma-Aldrich, Dorset, UK) were cultured in presence of fluorescently labeled Ti-CP4, Ti-6Al-4V and Ti-15Zr particles. Particles were functionalised and fluorescently labeled as described previously [21]: particles were dispersed in absolute ethanol (5 mg mL⁻¹) followed by careful addition of 28% ammonium hydroxide (5% v/v). (3-aminopropyl)triethoxysilane was then added into the solution (1:5) and left on an orbital shaker overnight at 200 rpm to complete the reactions. Amine functionalised particles were washed with absolute ethanol before labelling with fluorescein 5(6)-isothiocyanate (FITC). 1 mg mL⁻¹ FITC (dissolved in absolute ethanol) was mixed with amine functionalised particles and left on an orbital shaker for 16 h at 200 rpm. The weight ratio between particle and FITC was kept at 1:1. FITC labeled particles were washed in absolute ethanol and de-ionized water followed by sterilisation in 70% (v/v) ethanol.

HGFs and RAW 264.7 cells were seeded in tissue culture μ -dishes (35 mm diameter, ibidi®, Thistle Scientific Ltd, Glasgow, UK) at a density of 300 cells cm⁻². Cells were

allowed to grow in Dulbecco's modified Eagle's medium (DMEM) supplemented with 100 unit mL⁻¹ penicillin, 100 μ g mL⁻¹ streptomycin and 10% (v/v) foetal bovine serum (FBS) for 24 h in an humidified atmosphere containing 5% CO₂. Cells were then cultured overnight (16 h) in the presence of 250 μ g mL⁻¹ FITC labeled particles before fixation in 4% paraformaldehyde in PBS.

2.7.2. F-actin staining

F-actin was labeled using CytoPainter F-actin staining kit (Abcam, Cambridge, UK) following the manufacturer's instruction. Briefly, fixed cells were washed with PBS and incubated with Alexa Fluor® 568-conjugated phalloidin (1:1000 dilution in labelling buffer) for 1 h at room temperature. All samples were counter-stained with DAPI (0.1 μ g mL⁻¹ in PBS).

2.7.3. Confocal microscopy

Stained samples were imaged under confocal microscopy (Leica SP5 MP laser scanning confocal microscope and software, Leica Microsystems, Wetzlar, Germany). Fiji ImageJ software (version 1.52p, NIH, USA) was used for the processing and generation of orthogonal view interpolations. No further image adjustment, enhancement or filtering was applied.

2.8. Statistical analyses

Results were presented as mean \pm standard deviation (S.D.). Statistical analyses including non-parametric t-test (2 groups) and Kruskal-Wallis test with Dunn's post test (3 or more groups) using Prism 8 (GraphPad Software, US). Results were deemed significant if the probability of occurrence by random chance alone was less than 5% (i.e. $p < 0.05$).

3. Results

3.1. Metallic element release following placement of implants in pig mandible ex vivo model

Ti, V and Zr were not detected in bone and drilled bone controls. Ti was detected in bone samples following the placement of all types of implants, while V and Zr were detected only in the bone that had implants made of alloys containing

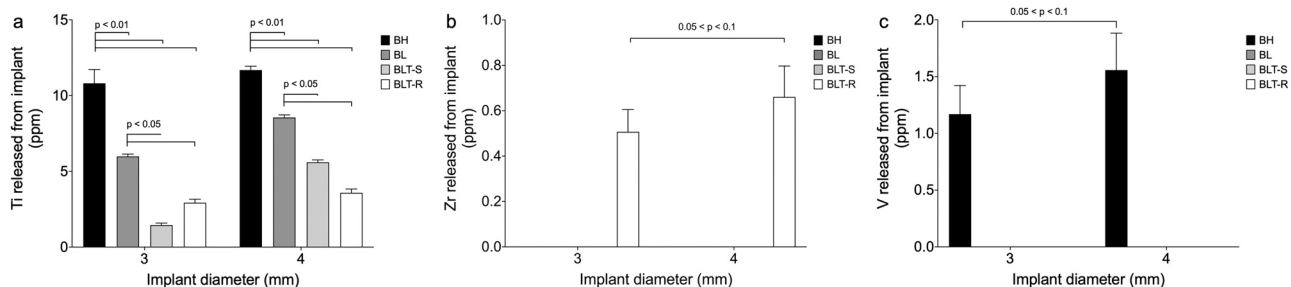


Fig. 2 – Elemental concentrations of Ti (a), Zr (b) and V (c) in bone sections as a result of implant placement and removal, measured by ICP-OES of digested bone. Results presented as mean \pm standard deviation ($n = 5$). Non-parametric t-test and Kruskal-Wallis test with Dunn's post test were used for comparisons between implant body design and materials respectively. p values are labeled on each graph. BL, BLT-S, BLT-R and BH are defined in Table 1.

those elements (Fig. 2). The amount of metallic species detected by ICP was dependent on implant diameter, implant body design as well as the material composition. For Ti-CP4 implants, larger implant diameter resulted in an increase in Ti detected in the bone by ICP (4 mm BL and BLT-S implants released 8.6 ± 0.2 and 5.6 ± 0.2 ppm Ti respectively in comparison to 6.0 ± 0.2 and 1.5 ± 0.1 ppm released by their 3 mm counter parts). Cylindrical body design (BL) released significantly more Ti (8.6 ± 0.2 and 6.0 ± 0.2 ppm respectively for 4 mm and 3 mm implants) in comparison to their tapered counterparts (BLT-S, 5.6 ± 0.2 and 1.5 ± 0.1 ppm respectively for 4 mm and 3 mm implants) with the same material and diameter.

For BLT-R (Ti-15Zr) implants, Ti release was not significantly affected by implant diameter (2.9 ± 0.2 and 3.5 ± 0.2 ppm for 3 and 4 mm diameter implants respectively). Zr release appeared to increase ($0.05 < p < 0.1$) with implant diameter, where 4 mm diameter implants resulted in 0.7 ± 0.1 ppm of Zr compared to 0.5 ± 0.1 ppm from 3 mm diameter implants. There was no significant difference in Ti ion release between BLT-S (Ti-CP4) and BLT-R (Ti-15Zr) implants, both of which have apically tapered body design. BH (Ti-6Al-4V) implants released significantly more Ti than the Ti-CP4 and Ti-15Zr implants, but Ti and V release were not significantly affected by implant diameter (10.8 ± 0.9 and 11.7 ± 0.3 ppm Ti and 1.2 ± 0.2 and 1.6 ± 0.3 for 3 and 4 mm diameter implants respectively).

A standard curve of Ti release against known quantity of implant particles were generated (Supplementary Fig. S2). The Ti contents (in ppm) obtained in Fig. 2 were input into the standard curve for the approximation of the quantities of materials lost (in μg) following implantation (Table 1). The observations were reminiscent of those from ICP results, where Ti-6Al-4V implants had most material loss following the mock ex-vivo placement and removal procedures. The estimated weight of material loss is listed in Table 1.

3.2. SEM and μ -CT imaging

SEM images were obtained in order to examine implant surface topography following placement and removal (Fig. 3). The apex, center and neck regions of each implant were imaged. Irregular grooves and metal fragments were observed on all implant surfaces, including those of as received implants (without implant placement and removal). Noticeable cracks were observed on alloyed implants including both BH and BLT-R implants following implant placement. Biological materials such as bone fragments were present on implants that had been inserted. μ -CT was used to visualise particles embedded in bone samples following placement and removal (Fig. 4). The maximum resolution of the scanner was $12 \mu\text{m}$ per voxel, hence only larger particles could be visualised. Particles were observed in bone samples placed with BH3, BH4, BL3 and BLT-S3 implants, however few particles were observed in each volume of interest (field of view).

3.3. Internalization of implant particles by cell

To demonstrate that particles released from dental implants can be internalized by peri-implant cell populations, human

gingival fibroblasts (HGFs) and RAW 264.7 murine macrophages were cultured in the presence of particles of Ti-CP4, Ti-6Al-4V or Ti-15Zr at $250 \mu\text{g mL}^{-1}$ for 16 h. The diameters of Ti-CP4, Ti-6Al-4V and Ti-15Zr were 34.1 ± 3.8 ($D50 = 32.2$), 33.3 ± 4.4 ($D50 = 30.3$) and 97.8 ± 8.2 ($D50 = 85.2$) μm respectively. DLS (dynamic light scattering) analysis showed nano-sized particles were also present, diameters of Ti-CP4, Ti-6Al-4V and Ti-15Zr were 95.4 ± 9.1 nm (modal number 79.3 nm), 77.74 ± 10.4 nm (modal number 70.1 nm) and 135.1 ± 11.3 nm (modal number 86.8 nm) respectively. Orthogonal view created using z-stacks obtained from confocal microscopy revealed that all 3 types of particles can be seen internalized by both HGFs and RAW 264.7 cells and were located mostly in cytoplasm (Fig. 5).

4. Discussion

The aim was to investigate the impact of dental implant composition, geometry and dimension on the release of particulates and metallic elements following implant placement. Dental implants used in this study include: BH (Ti-6Al-4V, tapered), BL (Ti-CP4, cylindrical), BLT-S (Ti-CP4, tapered) and BLT-R (Ti-15Zr, tapered). Both 3 and 4 mm variation of each implant were also included. Although debris can be generated from bone-cutting instruments during implant bed preparation, this can be mitigated by practices such as sufficient irrigation and suction as well as frequent use and replacement of harder single-use drills [22]. Hence the current study focused on the wear during implant placement. During implant placement, an initial interlocking was formed between the implant walls/threads and the peri-implant bone, in which microfractures and compression can occur at the bone side and at the same time, implant surface experience a combination of torsional and frictional forces [22]. The release of metallic species into the bone is believed to originate from two sources: firstly, the physical/mechanical damage to the implant surface (e.g. oxidation layer) during insertion, causing loss of fine particulates; and secondly, the dissolution of the subjacent material into the peri-implant tissues; resulting in detection of the both implant particles and ions in the bone [22,23]. As shown in Fig. 2, out of the three implant materials (Ti-CP4, Ti-6Al-4V and Ti-15Zr), Ti-6Al-4V implants released the highest amount ($p < 0.01$) of Ti following placement regardless of implant geometry and dimension. Poor tribological performance with low surface hardness has been reported for titanium alloys without surface modifications [24,25]. Grade 5 Ti-6Al-4V alloy is a dual alpha/beta phase alloy, in which vanadium is added to stabilise the larger beta phase, thus improving the mechanical properties, however, it has been shown that Ti-6Al-4V alloy inherently is more susceptible to corrosion [26,27]. When exposed to oxidative environment, Ti alloys, particularly Ti-6Al-4V, rapidly form an oxide layer on the surface due to their high reactivity [28]. The disruption and/or removal of this protective oxidative layer, typically during the mechanical contact between titanium alloys (or a titanium alloy and another material such as bone), may lead to increased wear damage in comparison to Ti-CP4 [28,29].

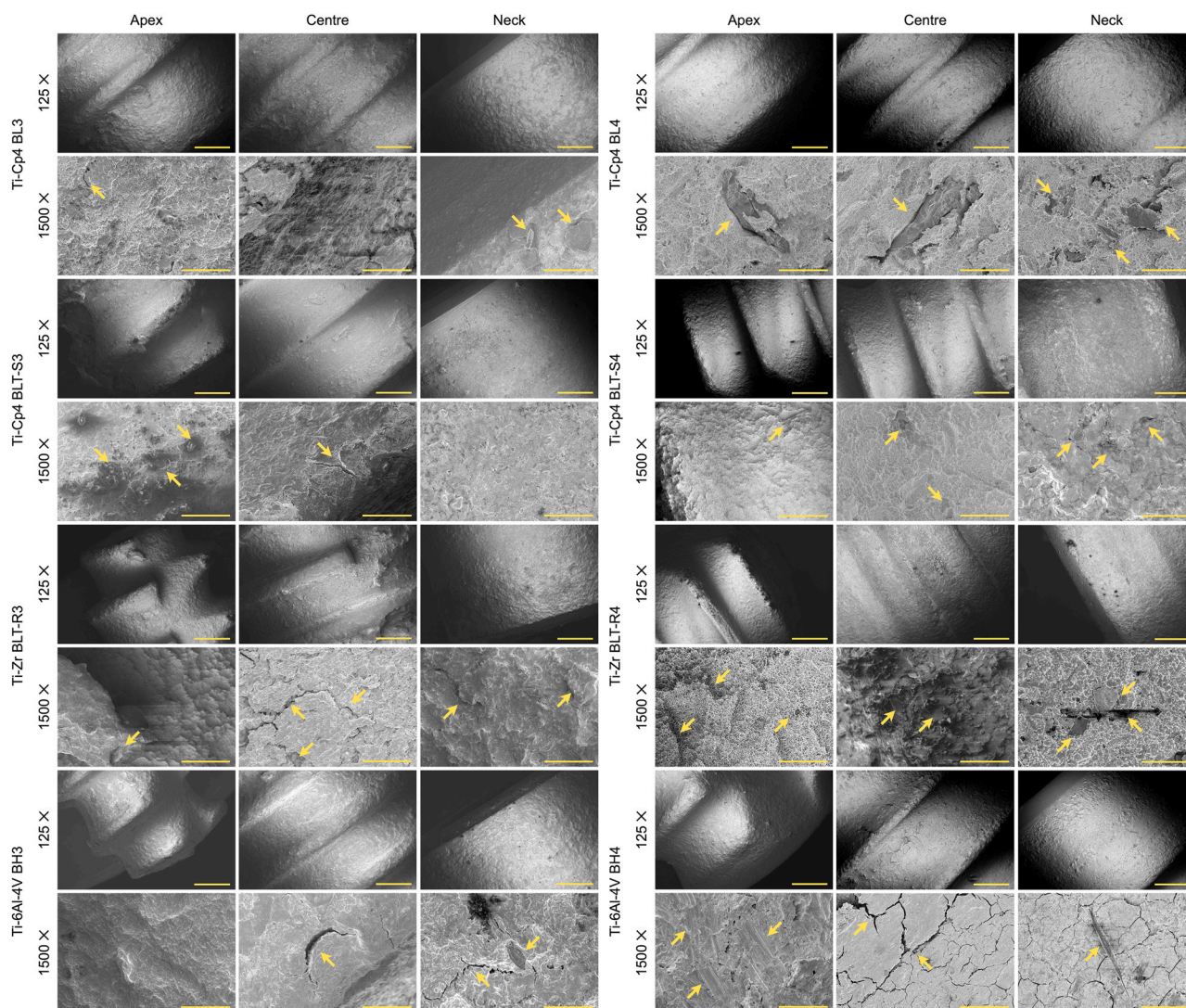


Fig. 3 – Representative SEM images of implants following placement and removal. The apex, center and neck regions of each implant were imaged. Fresh Ti-Cp4 and Ti-6Al-4V implants (controls) were also imaged (shown in [Supplementary Fig. S1](#)). Irregular grooves and metal fragments can be observed on all implant surfaces. Arrows indicate peelings and cracks can also be observed on alloy implants including both BH and BLT-R implants. Biological materials such as bone fragments are visible. Scale bars for 125 and 1500 × magnification are 500 and 50 μm respectively.

For metallic implants, increased wear rates have previously been shown in “wet” conditions, e.g. simulated body fluid environments, in comparison to atmospheric conditions, owing to the corrosive nature of the body fluid environments [29,30]. Sivakumar et al. compared the fretting corrosion behavior between Ti-6Al-4V alloy and Ti-Cp (unknown grade) in Ringer’s solution [29]. Although both Ti-6Al-4V alloy and Ti-Cp had similar wear morphology and change in free corrosion potential following a “ball-on-flat” wear configuration, Ti-6Al-4V demonstrated an increase in corrosion susceptibility, decrease in tendency for repassivation (growth of passive oxide layer in the fretted zone) and higher amount of wear volume in comparison to Ti-Cp. While fretting does not accurately represent implant placement or in vivo settings, the body of evidence from literature, in combination with the results presented here (Fig. 2 and Table 2),

can however be used to infer that the significantly increased Ti release from BH (Ti-6Al-4V) implants, in comparison to all other tested samples, was at least due in part to its corrosion susceptibility.

Roxid titanium zirconium alloy (Ti-15Zr) is a proprietary alloy, developed by Straumann, containing up to 15% Zr. It has been reported that dental implants manufactured using Ti-15Zr alloy have elastic characteristics (Young’s modulus between 102 and 104.7 GPa and Poisson coefficient of 0.33) very similar to grade 5 Ti-6Al-4V alloy [31]. The tensile strength of Ti-15Zr alloy (953 MPa) is higher than both Ti-6Al-4V (680 MPa) and Ti-Cp (310 MPa, unspecified grade) [31]. Titanium zirconium alloys have a binary alpha structure due to the near identical transformation behavior and very similar phase transition temperature between zirconium and titanium [32]. Due to this improved mechanical properties, Ti-

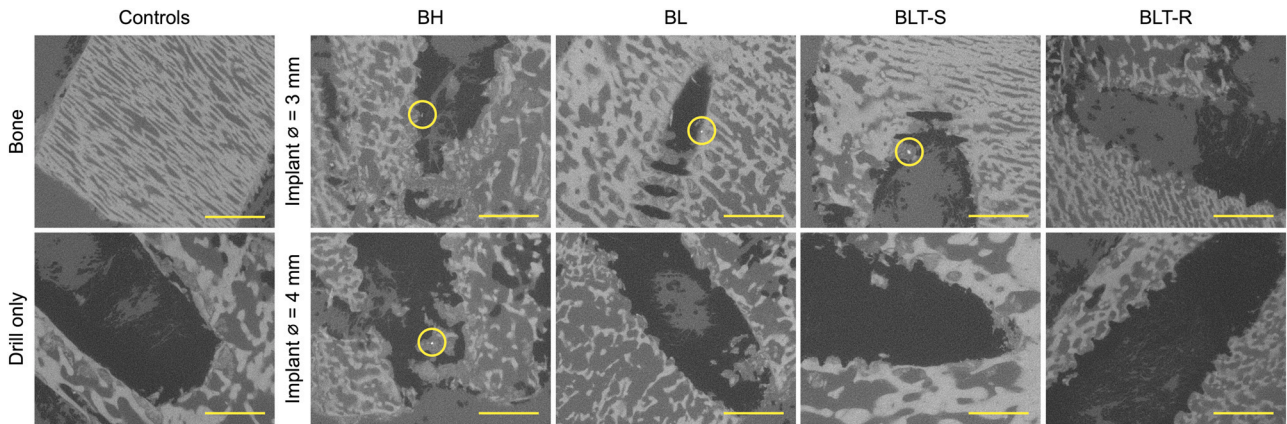


Fig. 4 – Representative sectional representation of micro-computed tomography images of bone samples following implant placement and removal. As indicated by yellow circles, pixel(s) attenuating at a much higher value (white or near white) suggest a possible metallic composition in contrast to bone tissue. Scale bars for bone and drill only controls are 5 mm. Scale bars are 2 mm.

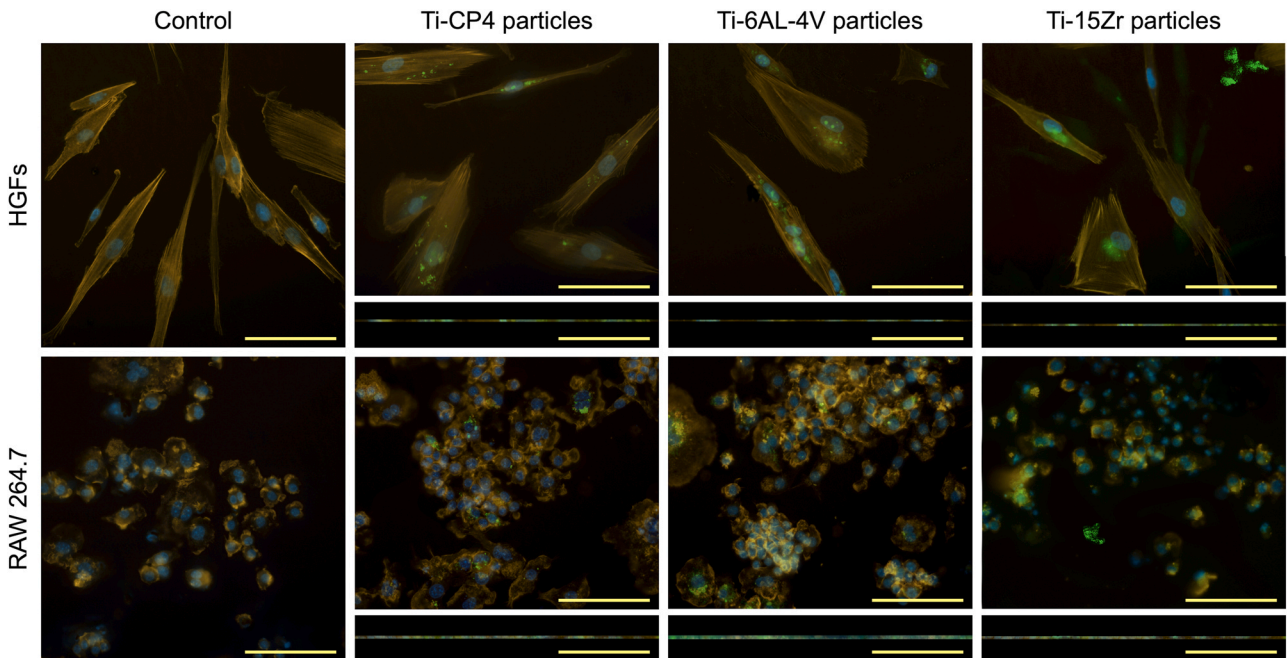


Fig. 5 – Representative confocal images of particles internalized by peri-implant cell populations. Yellow: Actin microfilaments, blue: cell nuclei and green: FITC functionalised particles. Orthogonal views were generated in Fiji ImageJ software (version 1.52p, NIH, USA). The diameters of Ti-CP4, Ti-6Al-4V and Ti-15Zr, as measured by Malvern Mastersizer, were 34.1 ± 3.8 ($D50 = 32.2$), 33.3 ± 4.4 ($D50 = 30.3$) and 97.8 ± 8.2 ($D50 = 85.2$) μm respectively. DLS analysis showed nano-sized particles were also present, diameters of Ti-CP4, Ti-6Al-4V and Ti-15Zr were 95.4 ± 9.1 nm ($D50 = 79.3$ nm), 77.74 ± 10.4 nm ($D50 = 70.1$ nm) and 135.1 ± 11.3 nm (modal number 86.8 nm) respectively. Scale bars are 100 μm .

15Zr was proposed for the manufacturing of narrow implants while reducing the risk of fracture. The fundamental advantages of a narrower implant include the possibility of maintaining a higher peri-implant bone volume and therefore the potential of long-term stability of peri-implant tissues [31]. Studies have also reported improved corrosion resistance of Ti-15Zr over Ti-6Al-4V alloy [32,33]. These phenomena could partially explain that the least amount of

metallic wear and ionic products were released from BLT-R (Ti-15Zr) implants in the current study.

As shown by the SEM images in Fig. 3, peelings and cracks can be observed on both BH (Ti-6Al-4V) and BLT-R (Ti-15Zr) alloyed implants following implant placement. As mentioned above, this could partially depend on the formation of oxide layer. This surface structural destruction could also be the result of surface modification. Although surface

modifications such as surface texturing and coating are becoming increasingly used by manufacturers in a bid to improve mechanical, tribological and biological properties, wear is still inevitable and further improvements to surface modification techniques are required [34]. We cannot comment on the effect of surface treatment on wear and ionic product release observed here without knowing the exact surface treatment applied to each tested implant samples here. It has been reported that surfaces with subtractive modification such as SLA (sand blasting and acid etching) suffer less wear and particle loosening [35,36]. In addition, there are other causes of wear following implant placement, such as abutment and implant body mechanical property mismatch [37], micro-gaps and movements [38], fluoride corrosion [39], bio-film formation [40], and interventions such as scaling and implantoplasty during maintenance [10,41], which were not investigated in the current study.

As shown in Fig. 2 and Table 1, regardless of implant material, there was a positive correlation between implant diameter and wear products release. Implants with cylindrical body design also appeared generated more material loss and metallic element release in comparison to their counterparts with apically tapered body design. One possible reason was due to the increase in implant-bone contact area in larger diameter and cylindrical implants. Authors did not tap the bone as per protocol for cylindrical implants in order to keep the same surgical procedure for all test implant samples, therefore that this could also lead to more shear force experienced by cylindrical implants than they are designed for. Nevertheless, similar observation has been previously reported and, in Orthopaedics, increased wear has been reported in metal-on-metal hip prostheses with larger dimensions [42,43]. It can also be observed from the SEM images in Fig. 3 that the damage varied along the implant with the tops at apex regions and some neck regions appear to be more damaged in comparison to those located at the implant body. This could be because apex is the region which first cut through the host bone. Previous studies also reported concentrations of metallic elements in the gingival cuff, surrounding the implant neck, as well as increased damage on some of the valleys of threads on implant body, owing to increased shear force and contact area at implant-bone interface [44,45].

In this study, the presence of implant particles in peri-implant bone tissues were detected using μ CT imaging (Fig. 4). Here, due to the limited resolution of the Zeiss Versa 520 X-Ray scanner (12.3 μ m per voxel) only particles with larger dimensions could be visualised. Previous studies have reported both nano- and micro- sized particles can be released from titanium based implants [5,10,46]. We did not use irrigation at the time of mock implant placement, so particle migration was not due to irrigation. Metallic particles and ions have been reported in intraoperative fluids, an evidence of release at the time of implant placement [47]. Metallic wear particle-induced aseptic implant loosening is a major concern after Orthopaedic surgery [48,49]. Different cell types, including monocytes, osteoblasts, and osteoclasts, are involved in this process. It has been reported that aseptic osteolysis can be induced by 0.2–3 mg of loose titanium particles (Ti-CP, unspecified grade) with extensive and non-

uniform osteoclast activity with increased bone resorption after 7 days [35,50,51]. As shown in Table 1, all tested implant systems resulted in material loss within or close to this range, hence further investigation with regards to the biological effects are needed. Metallic particles do not only present in peri-implant tissue but can also be internalized by cells. Cells cannot spread on small particles, but instead, the increased cell-titanium interaction tends to lead to membrane invagination around particles (nanoparticles in particular), resulting in their internalization and in turn interact with internal organelles and structures and subsequently cause functional modifications and intracellular lesions [16]. Here, all three types of particles were internalized by (Fig. 5) human gingival fibroblasts and RAW 264.7 macrophages, which were used as examples of typical cell populations that present in the dental peri-implant tissues. Previous study has demonstrated that particles from titanium and titanium based alloys can form bio-complexes (mixture of proteins and ions such as calcium and phosphorous) and enter cells via a “Trojan Horse”-like model [52]. Nano-sized particles released from metal implants are thought to enter cells via passive diffusion and in turn potentially result in biological responses at molecular level such as DNA methylation, histone post-translational modifications and noncoding RNAs in mammalian cells [10,46,53]. The exact mechanism and adverse effects that can be caused by the release of metallic particles and/or ionic products from a dental implant remain to be concluded: inflammatory tissue response, cytotoxicity, increased reactive oxygen species production, osteolysis and carcinogenesis are a few examples that have been recorded [17,46,54]. For Ti-6Al-4V alloys in particular, vanadium can elicit local as well as systemic mitochondrial- and cytotoxicity while aluminum has been reported to be associated with osteomalacia pulmonary granulomatosis and neurotoxicity [55,56]. While many in vitro, animal and clinical studies that focused on the biological effects of zirconium mainly showed a lack of adverse consequences, there are studies that reported changes in microRNAs (miRNAs) in response to exogenous elements including zirconium, suggesting possible epigenetic alterations (mitotically and meiotically heritable changes in gene expression that do not involve DNA sequence mutation) [57,58]. Some Zr-affected miRNAs such as miR-494 is involved in the regulation of tumorigenesis [59]. The exact biological/health effects of these miRNAs changes remain unclear. Without further systematic investigation, one cannot accurately recommend one material as the ideal implant material over the others, however, certain elements such as vanadium should be used with caution due to their well-documented adverse effects.

5. Conclusions

Metallic dental implants released particles and ions as a result of the procedure for insertion in an ex vivo pig mandible model. Implant composition and shape affected the amount of metal detected in the bone. Implants with wider body diameters and a cylindrical body design released more compared to their narrower and tapered body design counterparts. Ti-6Al-4V alloy released significantly more metallic

species in comparison to both Ti-CP4 and Ti-15Zr alloy counterparts with comparable design and dimensions. We have also demonstrated the internalization of metal particles by peri-implant cell populations including macrophages and human gingival fibroblasts. Future systematic investigation on the health effects from each available implant material are required.

Acknowledgments

Authors would like to thank Dr Shaaz Ghouse and Dr Jonathan Jeffers (Department of Mechanical Engineering, Imperial College London) for providing Ti-CP4 and Ti-6Al-4V particles. Authors would like to thank Straumann® (Basel, Switzerland) for providing Roxolid® (Ti-15Zr) disks.

Conflict of interests

The authors declare that they have no known competing financial interests or personal relationships that could have appeared to influence the work reported in this paper.

Funding Source

This research did not receive any specific grant from funding agencies in the public, commercial, or not-for-profit sectors.

Appendix A. Supporting information

Supplementary data associated with this article can be found in the online version at [doi:10.1016/j.dental.2022.04.003](https://doi.org/10.1016/j.dental.2022.04.003).

REFERENCES

- [1] Diebold U. The surface science of titanium dioxide. *Surf Sci Rep* 2003;48:53–229.
- [2] Moraschini V, Poubel LA, Ferreira VF, Barboza, Edos S. Evaluation of survival and success rates of dental implants reported in longitudinal studies with a follow-up period of at least 10 years: a systematic review. *Int J Oral Maxillofac Surg* 2015;44:377–88.
- [3] Revell PA. The combined role of wear particles, macrophages and lymphocytes in the loosening of total joint prostheses. *J R Soc Interface* 2008;5:1263–78.
- [4] Mathew MT, Srinivasa Pai P, Pourzal R, Fischer A, Wimmer MA. Significance of tribocorrosion in biomedical applications: overview and current status. *Adv Tribol* 2009;2009:250986/1–250986/12. <https://doi.org/10.1155/2009/250986:1-12>
- [5] Matusiewicz H. Potential release of in vivo trace metals from metallic medical implants in the human body: from ions to nanoparticles—a systematic analytical review. *Acta Biomater* 2014;10:2379–403.
- [6] Derks J, Tomasi C. Peri-implant health and disease. A systematic review of current epidemiology. *J Clin Periodont* 2015;42(Suppl 16):S158–71.
- [7] Esposito M, Grusovin MG, Worthington HV. Interventions for replacing missing teeth: treatment of peri-implantitis. *Cochrane Database Syst Rev* 2012;1:CD004970.
- [8] Konttinen YT, Pajarinen J, Takakubo Y, Gallo J, Nich C, Takagi M, et al. Macrophage polarization and activation in response to implant debris: influence by "particle disease" and "ion disease". *J Long Term Eff Med Implants* 2014;24:267–81.
- [9] Mombelli A, Hashim D, Cionca N. What is the impact of titanium particles and biocorrosion on implant survival and complications. *Clin Oral Implants Res* 2018;18:37–53. <https://doi.org/10.1111/clr.13305>
- [10] Barrak FN, Li S, Muntane AM, Jones JR. Particle release from implantoplasty of dental implants and impact on cells. *Int J Implant Dent* 2020;6:50.
- [11] Schlegel KA, Eppeneder S, Wiltfang J. Soft tissue findings above submerged titanium implants – a histological and spectroscopic study. *Biomaterials* 2002;23:2939–44.
- [12] Olmedo DG, Paparella ML, Spielberg M, Brandizzi D, Guglielmotti MB, Cabrini RL. Oral mucosa tissue response to titanium cover screws. *J Periodont* 2012;83:973–80.
- [13] Wawrzinek C, Sommer T, Fischer-Brandies H. Microdamage in cortical bone due to the overtightening of orthodontic microscrews. *J Orofac Orthop* 2008;69:121–34.
- [14] Guan H, van Staden RC, Johnson NW, Loo Y-C. Dynamic modelling and simulation of dental implant insertion process – a finiteelement study. *Finite Elem Anal Des* 2011;47:886–97.
- [15] de Moraes LS, Serra GG, Albuquerque Palermo EF, Andrade LR, Muller CA, Meyers MA, et al. Systemic levels of metallic ions released from orthodontic mini-implants. *Am J Orthod Dentofac Orthop* 2009;135:522–9.
- [16] Buzea C, Pacheco Ivan I, Robbie K. Nanomaterials and nanoparticles: sources and toxicity. *Biointerphases* 2007;2:MR17–71.
- [17] Eger M, Sterer N, Liron T, Kohavi D, Gabet Y. Scaling of titanium implants entrains inflammation-induced osteolysis. *Sci Rep* 2017;7:39612.
- [18] Nine MJ, Choudhury D, Hee AC, Mootanah R, Osman NAA. Wear debris characterization and corresponding biological response: artificial hip and knee joints. *Materials* 2014;7:980–1016.
- [19] Klinge B, Klinge A, Bertl K, Stavropoulos A. Peri-implant diseases. *Eur J Oral Sci* 2018;126(Suppl 1):88–94.
- [20] van Ginkel MF, van der Voet GB, de Wolff FA. Improved method of analysis for aluminum in brain tissue. *Clin Chem* 1990;36:658–61.
- [21] Naruphontjirakul P, Porter AE, Jones JR. In vitro osteogenesis by intracellular uptake of strontium containing bioactive glass nanoparticles. *Acta Biomater* 2018;66:67–80.
- [22] Delgado-Ruiz R, Romanos G. Potential causes of titanium particle and ion release in implant dentistry: a systematic review. *Int J Mol Sci* 2018;19.
- [23] Seki Y, Bessho K, Sugatani T, Kageyama T, Inui M, Tagawa T. Clinicopathological study on titanium miniplates. *J Oral Maxillofac Surg* 1994;40:892–6.
- [24] Frączek T, Olejnik M, Tokarz A. Evaluation of plasma nitriding efficiency of titanium alloys for medical applications. *METABK* 2009;48:83–6.
- [25] Textor M, Sittig C, Frauchiger V, Tosatti S, Brunette DM, Tengvall P, et al. Properties and biological significance of natural oxide films on titanium and its alloys. *The Effect of Hydrogen and Hydrides on the Integrity of Zirconium Alloy Components*. Springer Science and Business Media LLC; 2001. p. 171–230.
- [26] Jorge JR, Barao VA, Delben JA, Faverani LP, Queiroz TP, Assuncao WG. Titanium in dentistry: historical development, state of the art and future perspectives. *J Indian Prosthodont Soc* 2013;13:71–7.
- [27] Kuphasuk C, Oshida Y, Andres CJ, Hovijitra ST, Barco MT, Brown DT. Electrochemical corrosion of titanium and titanium-based alloys. *J Prosthet Dent* 2001;85:195–202.
- [28] Fellah M, Labaiz M, Assala O, Dekhil L, Taleb A, Rezag H, et al. Tribological behavior of Ti-6Al-4V and Ti-6Al-7Nb alloys for total hip prosthesis. *Adv Tribol* 2014;2014:1–13.

- [29] Sivakumar B, Kumar S, Sankara Narayanan TSN. Comparison of fretting corrosion behaviour of Ti–6Al–4V alloy and CP-Ti in Ringer’s solution. *Tribol Mater Surf Interfaces* 2011;5:158–64.
- [30] Ganesh BKC, Ramanaih N, Bhuvanewari N, Pammi SVN. Effect of Hank’s solution and shot blasting on the tribological behavior of titanium implant alloys. *Int J Mater Biomater Appl* 2012;2:5–11.
- [31] Brizuela-Velasco A, Pérez-Pevida E, Jiménez-Garrudo A, Gil-Mur FJ, Manero JM, Punset-Fuste M, et al. Mechanical characterisation and biomechanical and biological behaviours of Ti-Zr binary-alloy dental implants. *BioMed Res Int* 2017;2017:10.
- [32] Grandin HM, Berner S, Dard M. A review of titanium zirconium (TiZr) alloys for use in endosseous dental implants. *Materials* 2012;5:1348–60.
- [33] Correa DR, Vicente FB, Donato TA, Arana-Chavez VE, Buzalaf MA, Grandini CR. The effect of the solute on the structure, selected mechanical properties, and biocompatibility of Ti-Zr system alloys for dental applications. *Mater Sci Eng C Mater Biol Appl* 2014;34:354–9.
- [34] Ghosh S, Abanteriba S. Status of surface modification techniques for artificial hip implants. *Sci Technol Adv Mater* 2016;17:715–35.
- [35] Senna P, Antoninha Del Bel Cury A, Kates S, Meirelles L. Surface damage on dental implants with release of loose particles after insertion into bone. *Clin Implant Dent Relat Res* 2015;17:681–92.
- [36] Deppe H, Grunberg C, Thomas M, Sculean A, Benner KU, Bauer FJ. Surface morphology analysis of dental implants following insertion into bone using scanning electron microscopy: a pilot study. *Clin Oral Implants Res* 2015;26:1261–6.
- [37] Adachi K, Hutchings IM. Wear-mode mapping for the micro-scale abrasion test. *Wear* 2003;255:23–9.
- [38] Lopes PA, Carreira AFP, Nascimento RM, Vahey BR, Henriques B, Souza JCM. Physicochemical and microscopic characterization of implant-abutment joints. *Eur J Dent* 2018;12:100–4.
- [39] Schiff N, Grosogeat B, Lissac M, Dalard F. Influence of fluoride content and pH on the corrosion resistance of titanium and its alloys. *Biomaterials* 2002;23:1995–2002.
- [40] Prado AM, Pereira J, Henriques B, Benfatti CA, Magini RS, Lopez-Lopez J, et al. Biofilm affecting the mechanical integrity of implant-abutment joints. *Int J Prosthodont* 2016;29:381–3.
- [41] Claffey N, Clarke E, Polyzois I, Renvert S. Surgical treatment of peri-implantitis. *J Clin Periodontol* 2008;35:316–32.
- [42] Pettersson M, Pettersson J, Molin Thoren M, Johansson A. Release of titanium after insertion of dental implants with different surface characteristics - an ex vivo animal study. *Acta Biomater Odontol Scand* 2017;3:63–73.
- [43] Gill HS, Grammatopoulos G, Adshear S, Tsiologiannis E, Tsiridis E. Molecular and immune toxicity of CoCr nanoparticles in MoM hip arthroplasty. *Trends Mol Med* 2012;18:145–55.
- [44] Zabala A, Blunt L, Tejero R, Llavori I, Aginagalde A, Tato W. Quantification of dental implant surface wear and topographical modification generated during insertion. *Surf Topogr: Metrol Prop* 2020;8:015002.
- [45] Flatebo RS, Hol PJ, Leknes KN, Kosler J, Lie SA, Gjerdet NR. Mapping of titanium particles in peri-implant oral mucosa by laser ablation inductively coupled plasma mass spectrometry and high-resolution optical darkfield microscopy. *J Oral Pathol Med* 2011;40:412–20.
- [46] Bressan E, Ferroni L, Gardin C, Bellin G, Sbriccoli L, Sivolella S, et al. Metal nanoparticles released from dental implant surfaces: potential contribution to chronic inflammation and peri-implant bone loss. *Materials* 2019;12.
- [47] Cundy WJ, Mascarenhas AR, Antoniou G, Freeman BJ, Cundy PJ. Local and systemic metal ion release occurs intraoperatively during correction and instrumented spinal fusion for scoliosis. *J Child Orthop* 2015;9:39–43.
- [48] Hallab NJ, Jacobs JJ. Chemokines associated with pathologic responses to orthopedic implant debris. *Front Endocrinol (Lausanne)* 2017:8.
- [49] Landgraaber S, Jager M, Jacobs JJ, Hallab NJ. The pathology of orthopedic implant failure is mediated by innate immune system cytokines. *Mediat Inflamm* 2014;2014:185150.
- [50] Kaar SG, Ragab AA, Kaye SJ, Kilic BA, Jinnou T, Goldberg VM, et al. Rapid repair of titanium particle-induced osteolysis is dramatically reduced in aged mice. *J Orthop Res* 2001;19:171–8.
- [51] Shin DK, Kim MH, Lee SH, Kim TH, Kim SY. Inhibitory effects of luteolin on titanium particle-induced osteolysis in a mouse model. *Acta Biomater* 2012;8:3524–31.
- [52] Ribeiro AR, Gemini-Piperni S, Travassos R, Lemgruber L, Silva RC, Rossi AL, et al. Trojan-like internalization of anatase titanium dioxide nanoparticles by human osteoblast cells. *Sci Rep* 2016;6:23615.
- [53] Sierra MI, Valdes A, Fernandez AF, Torrecillas R, Fraga MF. The effect of exposure to nanoparticles and nanomaterials on the mammalian epigenome. *Int J Nanomed* 2016;11:6297–306.
- [54] Geetha M, Singh AK, Asokamani R, Gogia AK. Ti based biomaterials, the ultimate choice for orthopaedic implants – a review. *Prog Mater Sci* 2009;54:397–425.
- [55] Khadija G, Saleem A, Akhtar Z, Naqvi Z, Gull M, Masood M, et al. Short term exposure to titanium, aluminum and vanadium (Ti 6Al 4V) alloy powder drastically affects behavior and antioxidant metabolites in vital organs of male albino mice. *Toxicol Rep* 2018;5:765–70.
- [56] Kim KT, Eo MY, Nguyen TTH, Kim SM. General review of titanium toxicity. *Int J Implant Dent* 2019;5:10.
- [57] Kohal RJ, Schwindling FS, Bachle M, Spies BC. Peri-implant bone response to retrieved human zirconia oral implants after a 4-year loading period: a histologic and histomorphometric evaluation of 22 cases. *J Biomed Mater Res B Appl Biomater* 2016;104:1622–31.
- [58] Cossellu G, Motta V, Dioni L, Angelici L, Vigna L, Farronato G, et al. Titanium and zirconium levels are associated with changes in MicroRNAs expression: results from a human cross-sectional study on obese population. *PLOS One* 2016;11:e0161916.
- [59] Zhang Y, Guo L, Li Y, Feng GH, Teng F, Li W, et al. MicroRNA-494 promotes cancer progression and targets adenomatous polyposis coli in colorectal cancer. *Mol Cancer* 2018;17:1.